7-1-2004

Evidence for a Narrow Baryonic State Decaying to $K_S^0 p$ and $K_S^0 \bar{p}$ in Deep Inelastic Scattering at HERA

S. Chekanov
Argonne National Laboratory

M. Derrick
Argonne National Laboratory

J. H. Loizides
Argonne National Laboratory

S. Magill
Argonne National Laboratory

S. Miglioranzi
Argonne National Laboratory

Available online at www.sciencedirect.com
SCIENCE DIRECT®
Physics Letters B 591 (2004) 7–22
PHYSICS LETTERS B
www.elsevier.com/locate/physletb

Evidence for a narrow baryonic state decaying to $K^0_S p$ and $K^0_S \bar{p}$ in deep inelastic scattering at HERA

ZEUS Collaboration

S. Chekanov, M. Derrick, J.H. Loizides [1], S. Magill, S. Miglioranzi [1], B. Musgrave, J. Repond, R. Yoshida

Argonne National Laboratory, Argonne, IL 60439-4815, USA [40]

M.C.K. Mattingly

Andrews University, Berrien Springs, MI 49104-0380, USA

N. Pavel

Institut für Physik der Humboldt-Universität zu Berlin, Berlin, Germany

P. Antonioli, G. Bari, M. Basile, L. Bellagamba, D. Boscherini, A. Bruni, G. Bruni, G. Cara Romeo, L. Cifarelli, F. Cindolo, A. Contin, M. Corradi, S. De Pasquale, P. Giusti, G. Iacobucci, A. Margotti, A. Montanari, R. Nania, F. Palmonari, A. Pesci, L. Rinaldi, G. Sartorelli, A. Zichichi

University and INFN Bologna, Bologna, Italy [31]

G. Aghuzumtsyan, D. Bartsch, I. Brock, S. Goers, H. Hartmann, E. Hilger, P. Irrgang, H.-P. Jakob, O. Kind, U. Meyer, E. Paul [2], J. Rautenberg, R. Renner, A. Stifutkin, J. Tandler [3], K.C. Voss, M. Wang

Physikalisches Institut der Universität Bonn, Bonn, Germany [28]

D.S. Bailey [4], N.H. Brook, J.E. Cole, G.P. Heath, T. Namsoo, S. Robins, M. Wing

H.H. Wills Physics Laboratory, University of Bristol, Bristol, United Kingdom [39]

doi:10.1016/j.physletb.2004.04.024

M. Capua, A. Mastroberardino, M. Schioppa, G. Susinno

Physics Department, Calabria University, and INFN, Cosenza, Italy [31]

J.Y. Kim, I.T. Lim, K.J. Ma, M.Y. Pac [5]

Chonnam National University, Kwangju, South Korea [33]

M. Helbich, Y. Ning, Z. Ren, W.B. Schmidke, F. Sciulli

Nevis Laboratories, Columbia University, Irvington on Hudson, NY 10027, USA [41]

J. Chwastowski, A. Eskreys, J. Figiel, A. Galas, K. Olkiewicz, P. Stopa, L. Zawiejski

Institute of Nuclear Physics, Cracow, Poland [35]

L. Adamczyk, T. Bołd, I. Grabowska-Bołd [6], D. Kisielewska, A.M. Kowal, M. Kowal, J. Łukasik, M. Przybycień, L. Suszycki, D. Szuba, J. Szuba [7]

Faculty of Physics and Nuclear Techniques, AGH-University of Science and Technology, Cracow, Poland [42]

A. Kotański [8], W. Słomiński

Department of Physics, Jagellonian University, Cracow, Poland

V. Adler, U. Behrens, I. Bloch, K. Borras, V. Chiochia, D. Dannheim [9], G. Drews, J. Fourletova, U. Fricke, A. Geiser, P. Göttlicher [10], O. Gutsche, T. Haas, W. Hain, S. Hillert [11], C. Horn, B. Kahle, U. Kötz, H. Kowalski, G. Kramberger, H. Labes, D. Lelas, H. Lim, B. Löhr, R. Mankel, I.-A. Melzer-Pellmann, C.N. Nguyen, D. Notz, A.E. Nuncio-Quiroz, A. Polini, A. Raval, L. Rurua, U. Schneekloth, U. Stösslein, G. Wolf, C. Youngman, W. Zeuner

Deutsches Elektronen-Synchrotron DESY, Hamburg, Germany

S. Schlenstedt

DESY Zeuthen, Zeuthen, Germany

G. Barbagli, E. Gallo, C. Genta, P.G. Pelfer

University and INFN, Florence, Italy [31]

A. Bamberger, A. Benen, F. Karstens, D. Dobur, N.N. Vlasov

Fakultät für Physik der Universität Freiburg i.Br., Freiburg i.Br., Germany [28]

M. Bell, P.J. Bussey, A.T. Doyle, J. Ferrando, J. Hamilton, S. Hanlon, D.H. Saxon, I.O. Skillicorn

Department of Physics and Astronomy, University of Glasgow, Glasgow, United Kingdom [39]

I. Gialas

Department of Engineering in Management and Finance, University of Aegean, Greece

T. Carli, T. Gosau, U. Holm, N. Krumnack, E. Lohrmann, M. Milite, H. Salehi, P. Schleper, T. Schörner-Sadenius, S. Stonjek [11], K. Wichmann, K. Wick, A. Ziegler, Ar. Ziegler

Institute of Experimental Physics, Hamburg University, Hamburg, Germany [28]

C. Collins-Tooth, C. Foudas, R. Gonçalo [12], K.R. Long, A.D. Tapper

High Energy Nuclear Physics Group, Imperial College London, London, United Kingdom [39]

P. Cloth, D. Filges

Forschungszentrum Jülich, Institut für Kernphysik, Jülich, Germany

M. Kataoka [13], K. Nagano, K. Tokushuku [14], S. Yamada, Y. Yamazaki

Institute of Particle and Nuclear Studies, KEK, Tsukuba, Japan [32]

A.N. Barakbaev, E.G. Boos, N.S. Pokrovskiy, B.O. Zhautykov

Institute of Physics and Technology of Ministry of Education and Science of Kazakhstan, Almaty, Kazakhstan

D. Son

Center for High Energy Physics, Kyungpook National University, Daegu, South Korea [33]

K. Piotrzkowski

Institut de Physique Nucléaire, Université Catholique de Louvain, Louvain-la-Neuve, Belgium

F. Barreiro, C. Glasman [15], O. González, L. Labarga, J. del Peso, E. Tassi, J. Terrón, M. Zambrana

Departamento de Física Teórica, Universidad Autónoma de Madrid, Madrid, Spain [38]

M. Barbi, F. Corriveau, S. Gliga, J. Lainesse, S. Padhi, D.G. Stairs, R. Walsh

Department of Physics, McGill University, Montréal, PQ, H3A 2T8 Canada [27]

T. Tsurugai

Faculty of General Education, Meiji Gakuin University, Yokohama, Japan [32]

A. Antonov, P. Danilov, B.A. Dolgoshein, D. Gladkov, V. Sosnovtsev, S. Suchkov

Moscow Engineering Physics Institute, Moscow, Russia [36]

R.K. Dementiev, P.F. Ermolov, I.I. Katkov, L.A. Khein, I.A. Korzhavina, V.A. Kuzmin, B.B. Levchenko, O.Yu. Lukina, A.S. Proskuryakov, L.M. Shcheglova, S.A. Zotkin

Institute of Nuclear Physics, Moscow State University, Moscow, Russia [37]

I. Abt, C. Büttner, A. Caldwell, X. Liu, J. Sutiak

Max-Planck-Institut für Physik, München, Germany

N. Coppola, S. Grijpink, E. Koffeman, P. Kooijman, E. Maddox, A. Pellegrino, S. Schagen, H. Tiecke, M. Vázquez, L. Wiggers, E. de Wolf

NIKHEF and University of Amsterdam, Amsterdam, Netherlands [34]

N. Brümmer, B. Bylsma, L.S. Durkin, T.Y. Ling

Physics Department, Ohio State University, Columbus, OH 43210, USA [40]

A.M. Cooper-Sarkar, A. Cottrell, R.C.E. Devenish, B. Foster, G. Grzelak, C. Gwenlan [16], T. Kohno, S. Patel, P.B. Straub, R. Walczak

Department of Physics, University of Oxford, Oxford, United Kingdom [39]

A. Bertolin, R. Brugnera, R. Carlin, F. Dal Corso, S. Dusini, A. Garfagnini, S. Limentani, A. Longhin, A. Parenti, M. Posocco, L. Stanco, M. Turcato

Dipartimento di Fisica dell' Università and INFN, Padova, Italy [31]

E.A. Heaphy, F. Metlica, B.Y. Oh, J.J. Whitmore [17]

Department of Physics, Pennsylvania State University, University Park, PA 16802, USA [41]

Y. Iga

Polytechnic University, Sagamihara, Japan [32]

G. D'Agostini, G. Marini, A. Nigro

Dipartimento di Fisica, Università 'La Sapienza' and INFN, Rome, Italy [31]

C. Cormack [18], J.C. Hart, N.A. McCubbin

Rutherford Appleton Laboratory, Chilton, Didcot, Oxon, United Kingdom [39]

C. Heusch

University of California, Santa Cruz, CA 95064, USA [40]

I.H. Park

Department of Physics, Ewha Womans University, Seoul, South Korea

H. Abramowicz, A. Gabareen, S. Kananov, A. Kreisel, A. Levy

Raymond and Beverly Sackler Faculty of Exact Sciences, School of Physics, Tel-Aviv University, Tel-Aviv, Israel [30]

M. Kuze

Department of Physics, Tokyo Institute of Technology, Tokyo, Japan [32]

T. Fusayasu, S. Kagawa, T. Tawara, T. Yamashita

Department of Physics, University of Tokyo, Tokyo, Japan [32]

R. Hamatsu, T. Hirose [2], M. Inuzuka, H. Kaji, S. Kitamura [19], K. Matsuzawa

Department of Physics, Tokyo Metropolitan University, Tokyo, Japan [32]

M. Costa, M.I. Ferrero, V. Monaco, R. Sacchi, A. Solano

Università di Torino and INFN, Torino, Italy [31]

M. Arneodo, M. Ruspa

Università del Piemonte Orientale, Novara, and INFN, Torino, Italy [31]

T. Koop, J.F. Martin, A. Mirea

Department of Physics, University of Toronto, Toronto, ON, M5S 1A7 Canada [27]

J.M. Butterworth [20], R. Hall-Wilton, T.W. Jones, M.S. Lightwood, M.R. Sutton [4], C. Targett-Adams

Physics and Astronomy Department, University College London, London, United Kingdom [39]

J. Ciborowski [21], R. Ciesielski [22], P. Łużniak [23], R.J. Nowak, J.M. Pawlak, J. Sztuk [24], T. Tymieniecka, A. Ukleja, J. Ukleja [25], A.F. Żarnecki

Institute of Experimental Physics, Warsaw University, Warsaw, Poland [43]

M. Adamus, P. Plucinski

Institute for Nuclear Studies, Warsaw, Poland [43]

Y. Eisenberg, D. Hochman, U. Karshon, M. Riveline

Department of Particle Physics, Weizmann Institute, Rehovot, Israel [29]

A. Everett, L.K. Gladilin [26], D. Kçira, S. Lammers, L. Li, D.D. Reeder, M. Rosin, P. Ryan, A.A. Savin, W.H. Smith

Department of Physics, University of Wisconsin, Madison, WI 53706, USA [40]

S. Dhawan

Department of Physics, Yale University, New Haven, CT 06520-8121, USA [40]

S. Bhadra, C.D. Catterall, S. Fourletov, G. Hartner, S. Menary, M. Soares, J. Standage

Department of Physics, York University, ON, M3J 1P3 Canada [27]

Received 30 March 2004; accepted 7 April 2004

Available online 12 May 2004

Editor: W.-D. Schlatter

Abstract

A resonance search has been made in the $K^0_S p$ and $K^0_S \bar{p}$ invariant-mass spectrum measured with the ZEUS detector at HERA using an integrated luminosity of 121 pb^{-1}. The search was performed in the central rapidity region of inclusive deep inelastic scattering at an ep centre-of-mass energy of 300–318 GeV for exchanged photon virtuality, Q^2, above 1 GeV^2. Recent results from fixed-target experiments give evidence for a narrow baryon resonance decaying to K^+n and $K^0_S p$, interpreted as a pentaquark. The results presented here support the existence of such state, with a mass of $1521.5 \pm 1.5(\text{stat.})^{+2.8}_{-1.7}(\text{syst.})$ MeV and a Gaussian width consistent with the experimental resolution of 2 MeV. The signal is visible at high Q^2 and, for $Q^2 > 20$ GeV^2, contains 221 ± 48 events. The probability of a similar signal anywhere in the range 1500–1560 MeV arising from fluctuations of the background is below 6×10^{-5}.

1. Introduction

Recent results from fixed-target experiments give evidence for the existence of a narrow baryon resonance with a mass of approximately 1530 MeV and positive strangeness [1],seen in the K^+n decay channel. These results have triggered new interest in baryon spectroscopy since this baryon is manifestly exotic; it cannot be composed of three quarks, but may be explained as a bound state of five quarks, i.e., as a pentaquark, $\Theta^+ = uudd\bar{s}$. A narrow baryonic resonance close to the observed mass is predicted in the chiral soliton model [2]. The quantum numbers of this state also permit decays to $K^0_S p$ and $K^0_S \bar{p}$ (denoted as $K^0_S p(\bar{p})$). Evidence for a corresponding signal has been seen [3] in this channel by other experiments. Evidence for two other pentaquark states has also been reported recently [4,5].

The Particle Data Group (PDG) [6] lists a number of 'Σ bumps', unestablished resonances observed with low significance by previous fixed-target experiments. The possible presence of these resonances in the mass region close to the production threshold of the $K^0_S p(\bar{p})$ final state complicates the search for pentaquarks in this decay channel.

The Θ^+ state and the Σ bumps discussed above have never been observed in high-energy experiments, where hadron production is dominated by fragmenta-

E-mail address: rik.yoshida@desy.de (R. Yoshida).
[1] Also affiliated with University College London, London, UK.
[2] Retired.
[3] Self-employed.
[4] PPARC Advanced fellow.
[5] Now at Dongshin University, Naju, South Korea.
[6] Partly supported by Polish Ministry of Scientific Research and Information Technology, grant No. 2P03B 12225.
[7] Partly supported by Polish Ministry of Scientific Research and Information Technology, grant No. 2P03B 12625.
[8] Supported by the Polish State Committee for Scientific Research, grant No. 2 P03B 09322.
[9] Now at Columbia University, NY, USA.
[10] Now at DESY group FEB.
[11] Now at University of Oxford, Oxford, UK.
[12] Now at Royal Holoway University of London, London, UK.
[13] Also at Nara Women's University, Nara, Japan.
[14] Also at University of Tokyo, Tokyo, Japan.
[15] Ramón y Cajal Fellow.
[16] PPARC Postdoctoral Research Fellow.
[17] On leave of absence at The National Science Foundation, Arlington, VA, USA.
[18] Now at University of London, Queen Mary College, London, UK.
[19] Present address: Tokyo Metropolitan University of Health Sciences, Tokyo 116-8551, Japan.
[20] Also at University of Hamburg, Alexander von Humboldt Fellow.
[21] Also at Łódź University, Poland.
[22] Supported by the Polish State Committee for Scientific Research, grant No. 2P03B 07222.
[23] Łódź University, Poland.
[24] Łódź University, Poland, supported by the KBN grant 2P03B12925.
[25] Supported by the KBN grant 2P03B12725.
[26] On leave from MSU, partly supported by the Weizmann Institute via the US–Israel BSF.
[27] Supported by the Natural Sciences and Engineering Research Council of Canada (NSERC).
[28] Supported by the German Federal Ministry for Education and Research (BMBF), under contract Nos. HZ1GUA 2, HZ1GUB 0, HZ1PDA 5, HZ1VFA 5.
[29] Supported by the MINERVA Gesellschaft für Forschung GmbH, the Israel Science Foundation, the US–Israel Binational Science Foundation and the Benozyio Center for High Energy Physics.
[30] Supported by the German–Israel Foundation and the Israel Science Foundation.
[31] Supported by the Italian National Institute for Nuclear Physics (INFN).
[32] Supported by the Japanese Ministry of Education, Culture, Sports, Science and Technology (MEXT) and its grants for Scientific Research.
[33] Supported by the Korean Ministry of Education and Korea Science and Engineering Foundation.
[34] Supported by the Netherlands Foundation for Research on Matter (FOM).
[35] Supported by the Polish State Committee for Scientific Research, grant No. 620/E-77/SPB/DESY/P-03/DZ 117/2003-2005.
[36] Partially supported by the German Federal Ministry for Education and Research (BMBF).
[37] Supported by RF President grant No. 1685.2003.2 for the leading scientific schools and by the Russian Ministry of Industry, Science and Technology through its grant for Scientific Research on High Energy Physics.
[38] Supported by the Spanish Ministry of Education and Science through funds provided by CICYT.
[39] Supported by the Particle Physics and Astronomy Research Council, UK.
[40] Supported by the US Department of Energy.
[41] Supported by the US National Science Foundation.
[42] Supported by the Polish Ministry of Scientific Research and Information Technology, grant No. 112/E-356/SPUB/DESY/P-03/DZ 116/2003-2005.
[43] Supported by the Polish State Committee for Scientific Research, grant No. 115/E-343/SPUB-M/DESY/P-03/DZ 121/2001-2002, 2 P03B 07022.

tion. This Letter presents the results of a search for narrow states in the $K^0_S p(\bar{p})$ decay channel in the central rapidity region of high-energy ep collisions, where particle production is not expected to be influenced by the baryon number in the initial state. The analysis was performed using deep inelastic scattering (DIS) events measured with exchanged-photon virtuality $Q^2 \geqslant 1$ GeV^2. The data sample, collected with the ZEUS detector at HERA, corresponds to an integrated luminosity of 121 pb^{-1}, taken between 1996 and 2000. This sample is the sum of 38 pb^{-1} of e^+p data taken at a centre-of-mass energy of 300 GeV and 68 pb^{-1} taken at 318 GeV, plus 16 pb^{-1} of e^-p data taken at 318 GeV.

2. Experimental set-up

A detailed description of the ZEUS detector can be found elsewhere [7]. A brief outline of the components that are most relevant for this analysis is given below.

Charged particles are tracked in the central tracking detector (CTD) [8], which operates in a magnetic field of 1.43 T provided by a thin superconducting solenoid. The CTD consists of 72 cylindrical drift chamber layers, organised in nine superlayers covering the polar-angle[44] region $15° < \theta < 164°$. The transverse-momentum resolution for full-length tracks is $\sigma(p_T)/p_T = 0.0058 p_T \oplus 0.0065 \oplus 0.0014/p_T$, with p_T in GeV. To estimate the ionization energy loss per unit length, dE/dx, of particles in the CTD [9], the truncated mean of the anode-wire pulse heights was calculated, which removes the lowest 10% and at least the highest 30% depending on the number of saturated hits. The measured dE/dx values were corrected by normalising to the average dE/dx for tracks around the region of minimum ionisation for pions, $0.3 < p < 0.4$ GeV. Henceforth, dE/dx is quoted in units of minimum ionising particles (mips). The dE/dx distribution for electrons has a roughly Gaussian shape centred about $dE/dx \sim 1.4$ mips with width 0.14 mips, corresponding to a resolution of $\sim 10\%$.

The high-resolution uranium-scintillator calorimeter (CAL) [10] consists of three parts: the forward, the barrel and the rear calorimeters. The smallest subdivision of the calorimeter is called a cell. The CAL energy resolutions, as measured under test-beam conditions, are $\sigma(E)/E = 0.18/\sqrt{E}$ for electrons and $\sigma(E)/E = 0.35/\sqrt{E}$ for hadrons, with E in GeV. A presampler [11] mounted in front of the calorimeter was used to correct the energy of the scattered electron.[45] The position of electrons scattered close to the electron beam direction is determined by a scintillator-strip detector [12].

The luminosity was measured using the bremsstrahlung process $ep \to ep\gamma$ with the luminosity monitor [13], a lead-scintillator calorimeter placed in the HERA tunnel at $Z = -107$ m.

3. Event simulation

Inclusive DIS events were generated using the ARIADNE 4.08 Monte Carlo (MC) model [14] interfaced with HERACLES 4.5.2 [15] via the DJANGOH 1.1 program [16] in order to incorporate first-order electroweak corrections. The ARIADNE program uses the Lund string model [17] for hadronisation, as implemented in JETSET 7.4 [18].

Before detector simulation, the $K^0_S p(\bar{p})$ invariant-mass distribution was calculated from the true K^0_S and (anti)protons in the mass range up to 1700 MeV. No peaks were found, indicating that no reflection from known decays are expected to generate a narrow peak in these decay channels.

The generated events were passed through a full simulation of the detector using GEANT 3.13 [19] and processed with the same reconstruction program as used for the data. The detector-level MC samples were then selected in the same way as the data. The generated MC statistics were about three times higher than those of the data.

4. Event sample

The search was performed using DIS events with $Q^2 \geqslant 1$ GeV^2, the largest event sample for which

[44] The ZEUS coordinate system is a right-handed Cartesian system, with the Z axis pointing in the proton beam direction, referred to as the "forward direction", and the X axis pointing left towards the centre of HERA. The coordinate origin is at the nominal interaction point.

[45] Henceforth the term electron is used to refer both to electrons and positrons.

no explicit trigger requirement was imposed on the hadronic final state. A three-level trigger [7] was used to select events online. At the third level, an electron with an energy greater than 4 GeV and a position outside a box of 24×12 cm^2 on the face of the calorimeter was required. The trigger has a high acceptance for $Q^2 \gtrsim 2$ GeV^2. However, data below $Q^2 \approx 20$ GeV^2 are strongly affected by prescales which were applied to the inclusive triggers to control data rates.

The Bjorken scaling variables x and y, as well as Q^2, were reconstructed using the electron method (denoted by the subscript e), which uses measurements of the energy and angle of the scattered electron, or using the Jacquet–Blondel (JB) method [20]. The scattered-electron candidate was identified from the pattern of energy deposits in the CAL [21].

The following requirements were imposed:

- $Q_e^2 \geqslant 1$ GeV^2;
- $E_{e'} \geqslant 8.5$ GeV, where $E_{e'}$ is the corrected energy of the scattered electron measured in the CAL;
- $35 \leqslant \delta \leqslant 60$ GeV, where $\delta = \sum E_i(1 - \cos\theta_i)$, E_i is the energy of the ith calorimeter cell, θ_i is its polar angle and the sum runs over all cells;
- $y_e \leqslant 0.95$ and $y_{\mathrm{JB}} \geqslant 0.01$;
- $|Z_{\mathrm{vertex}}| \leqslant 50$ cm, where Z_{vertex} is the vertex position determined from the tracks.

The present analysis is based on charged tracks measured in the CTD. The tracks were required to pass through at least five CTD superlayers and to have transverse momenta $p_T \geqslant 0.15$ GeV and pseudorapidity in the laboratory frame $|\eta| \leqslant 1.75$, restricting the study to a region where the CTD track acceptance and resolution are high. Candidates for long-lived neutral strange hadron decaying to two charged particles are identified by selecting pairs of oppositely charged tracks, fitted to a displaced secondary vertex. Events were required to have at least one such candidate.

After these selection cuts, a sample of 1 600 000 events remained.

5. Reconstruction of K_S^0 candidates

The K_S^0 mesons were identified by their charged-decay mode, $K_S^0 \to \pi^+\pi^-$. Both tracks were assigned the mass of the charged pion and the invariant mass, $M(\pi^+\pi^-)$, of each track pair was calculated. The K_S^0 candidates were selected by imposing the following requirements:

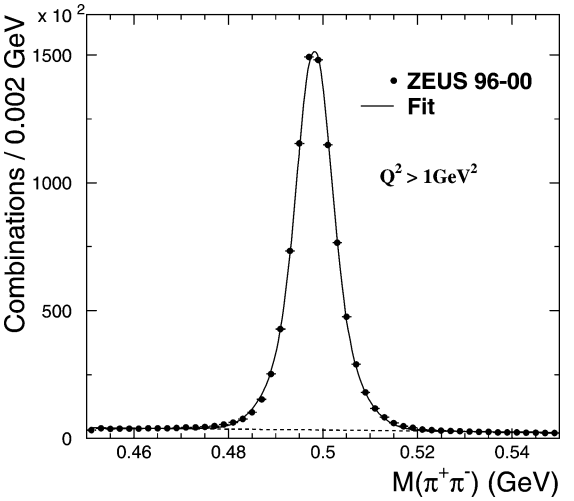

Fig. 1. The $\pi^+\pi^-$ invariant-mass distribution for $Q^2 > 1$ GeV^2. The solid line shows the fit result using a double Gaussian plus a linear background, while the dashed line shows the linear background.

- $M(e^+e^-) \geqslant 50$ MeV, where the electron mass was assigned to each track, to eliminate tracks from photon conversions;
- $M(p\pi) \geqslant 1121$ MeV, where the proton mass was assigned to the track with higher momentum, to eliminate Λ and $\bar{\Lambda}$ contamination of the K_S^0 signal;
- $483 \leqslant M(\pi^+\pi^-) \leqslant 513$ MeV;
- $p_T(K_S^0) \geqslant 0.3$ GeV and $|\eta(K_S^0)| \leqslant 1.5$.

Fig. 1 shows the invariant-mass distribution for K_S^0 candidates for $Q^2 \geqslant 1$ GeV^2. A fit using two Gaussian functions plus a first-order polynomial function was used. The number of K_S^0 candidates was $866\,800 \pm 1000$, with a background under the peak constituting approximately 6% of the total number of candidates. The peak position was $m_{K_S^0} = 498.12 \pm 0.01$(stat.) MeV, which agrees with the PDG value of 497.67 ± 0.03 [6] within the calibration uncertainty of the CTD. The width is consistent with the detector resolution.

6. Selection of $p(\bar{p})$ candidates

The (anti)proton candidate selection used the energy-loss measurement in the CTD, dE/dx. Fig. 2 shows the dE/dx distribution as a function of the track momentum for positive and negative tracks. Tracks fitted to the primary vertex were used, with the exception of the scattered-electron track. Tracks were selected as described in Section 4. In addition, only tracks with more than 40 CTD hits were used to ensure a good dE/dx measurement. The tracks were then selected by requiring $f \leqslant dE/dx \leqslant F$, where f and F, motivated by the Bethe–Bloch equation, are the functions: $f = 0.35/p^2 + 0.8$, $F = 1.0/p^2 + 1.2$ (for positive tracks) and $f = 0.3/p^2 + 0.8$, $F = 0.75/p^2 + 1.2$ (for negative tracks), where p is the total track momentum in GeV. These cuts were found from an examination of dE/dx as a function of p and were checked by studying (anti)proton candidate tracks from $\Lambda(\bar{\Lambda})$ decays. The proton band was found to be broader than that of the antiproton. There is also a clear deuteron band for positive tracks, which suggests a small contribution from secondary interactions. To remove the region where the proton band completely overlaps the pion band, the proton momentum was required to be less than 1.5 GeV. Finally, a cut requiring $dE/dx \geqslant 1.15$ mips was applied.

After these cuts, the purity of the proton sample, estimated from the MC simulation, is around 60%, varying from 96% at low momentum to 17% at the highest accepted momenta. Applying a higher dE/dx cut leads to higher purity, but reduces the acceptance for protons in the high-momentum region and reduces the statistics.

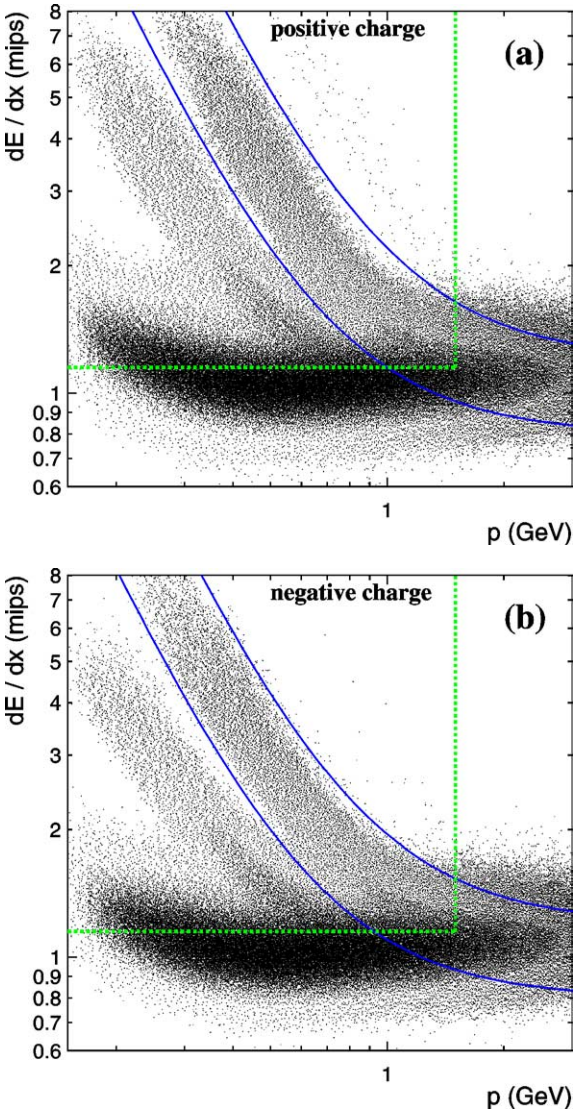

Fig. 2. The dE/dx distribution as a function of the track momentum for: (a) positive and (b) negative tracks. The dE/dx is normalised to a minimum ionising particle, defined as the average truncated mean of pion tracks in the momentum range $0.3 < p < 0.4$ GeV. The solid lines indicate the (anti)proton bands used in this analysis, and the dotted line denotes the cuts $dE/dx > 1.15$ mips and $p < 1.5$ GeV.

7. Reconstruction of $K^0_S p(\bar{p})$ invariant mass

The $K^0_S p(\bar{p})$ invariant mass was obtained by combining K^0_S and (anti)proton candidates selected as described above, and fixing the K^0_S mass to the PDG value. The resolution of the $K^0_S p(\bar{p})$ invariant-mass measurement was estimated using MC simulations to be 2.0 ± 0.5 MeV in the region near 1530 MeV, for both the $K^0_S p$ and the $K^0_S \bar{p}$ channels.

The resolution was independently verified from the data by reconstructing the $K^*(892)$ peak, assuming that the momentum and angle resolution for (anti)protons is similar to that for pions. Tracks passing the same angle and momentum cuts as the proton candidate sample were taken from the pion band, assigned the pion mass, and combined with the K^0_S candidates. A fit was performed using a Breit–Wigner function convoluted with a Gaussian to describe the

resolution. The width of the Breit–Wigner function was fixed to the natural width of the K^* resonance of 50.8 MeV [6]. The resulting width of the Gaussian was $5 \pm 2(\text{stat.})$ MeV, independent of the pion charge.

8. Results

The $K^0_S p(\bar{p})$ mass spectrum, in the range from threshold to 1700 MeV, is shown in Fig. 3 for various regions of the DIS phase space. Fig. 3(a)–(d) shows the mass distribution integrated above a minimum Q^2 ranging from 1 to 50 GeV^2. The data show signs of structure below about 1600 MeV. For $Q^2 >$ 10 GeV^2, a peak is seen in the mass distribution around 1520 MeV. Figs. 3(a) and (f) shows the $Q^2 >$ 1 GeV^2 sample divided into two bins of the photon–proton centre-of-mass energy, W. A peak is seen in the lower W bin.

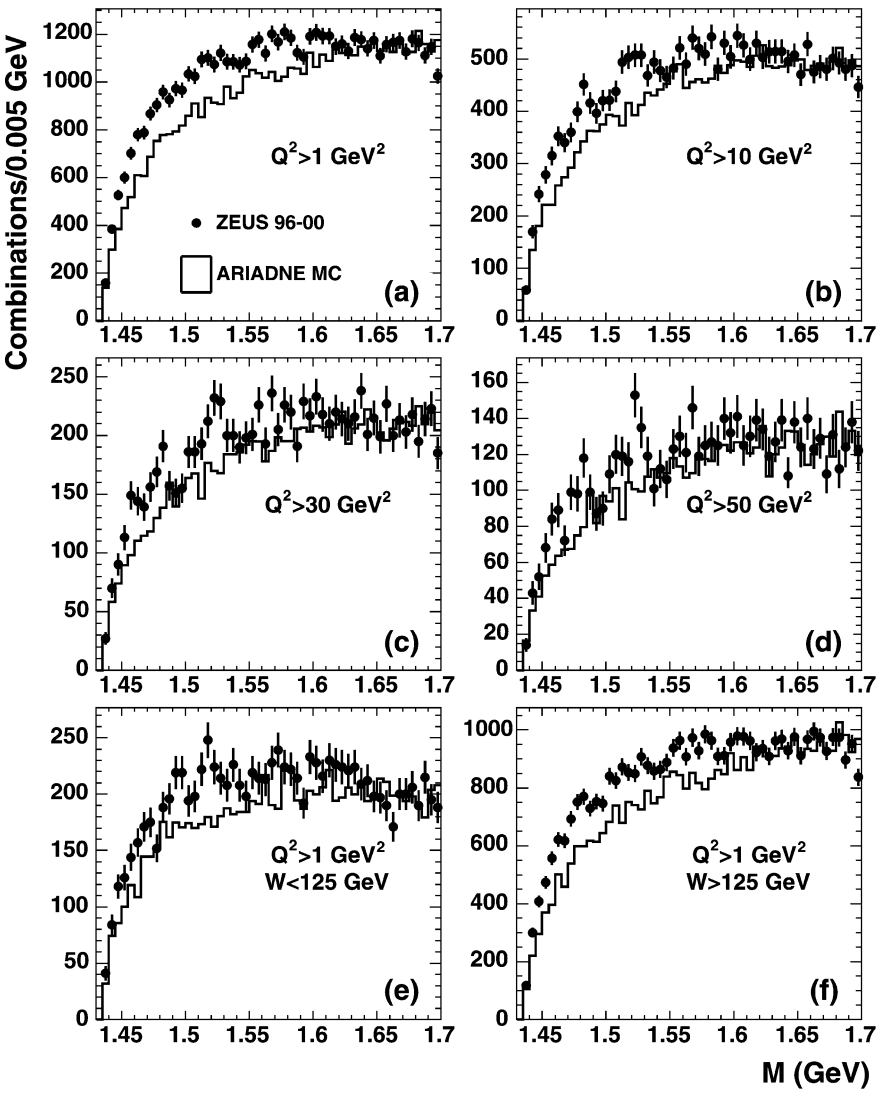

Fig. 3. Invariant-mass spectrum for the $K^0_S p(\bar{p})$ channel, after the cuts $f \leqslant dE/dx \leqslant F$, $dE/dx > 1.15$ mips and $p < 1.5$ GeV, integrated for (a) $Q^2 > 1$ GeV^2, (b) $Q^2 > 10$ GeV^2, (c) $Q^2 > 30$ GeV^2, (d) $Q^2 > 50$ GeV^2, (e) $Q^2 > 1$ GeV^2 and $W < 125$ GeV (f) $Q^2 > 1$ GeV^2 and $W > 125$ GeV. The histogram shows the prediction of the ARIADNE MC simulation normalised to the data in the mass region above 1650 MeV.

The expectation from the MC simulation, scaled to agree with the data in the mass region above 1650 MeV, is also shown. If normalised to the luminosity, the simulation lies below the data by a factor of approximately two (not shown). Even after scaling, the data are not well described by the simulation for masses below 1600 MeV, and no structure is seen in the simulated data. The PDG reports a Σ bump at 1480 MeV, and several states above 1550 MeV. None of these states are included in the simulation, which includes only well established resonances.

Several functional forms were fit to the data for $Q^2 > 20$ GeV^2 over the mass range from threshold up to 1700 MeV to estimate the significance of the peak, as well as its position and width. A background of the form

$$P_1(M - m_p - m_{K^0_S})^{P_2} \times \left(1 + P_3(M - m_p - m_{K^0_S})\right),$$

where M is the $K^0_S p(\bar{p})$ candidate mass, m_p and $m_{K^0_S}$ are the masses of the proton and the K^0_S, respectively, and P_1, P_2 and P_3 are parameters, was found to give a good description of the data when combined with Gaussians to describe the signal near 1520 MeV as well as possible contributions from Σ bumps. The parameters of the Gaussians and the background were left free. A bin-by-bin χ^2 minimisation was used. The results of the fit using the background function plus one and two Gaussians are shown in Table 1. Reducing the number of parameters in the background function significantly reduces the quality of the fit. Adding a third Gaussian does not significantly improve the fit. The result of the fit using two Gaussians is shown in Fig. 4. The second Gaussian significantly improves the fit in the low mass region, and has a mass of 1465.1 ± 2.9(stat.) MeV and a width of 15.5 ± 3.4(stat.) MeV and may correspond to the $\Sigma(1480)$. However, the parameters and significance of any state in this region are difficult to estimate due to the steeply falling background close to threshold. The signal peak position is 1521.5 ± 1.5(stat.) MeV, with a measured Gaussian width 6.1 ± 1.6(stat.) MeV, consistent with the resolution. The fit gives 221 ± 48 events above the background, corresponding to 4.6σ. The equivalent estimate for the single Gaussian fit is 3.9σ. The χ^2 per degree of freedom for the fit over the whole fitted range of masses is 35/44. Over the same range, the χ^2 per degree of freedom for the fit with no Gaussians is 69/50, which is an acceptable fit. However, this value is dominated by contributions from the high-mass region. A number of MC experiments were carried out, using the background fit with zero gaussians as a starting distribution and generating random data using Poisson statistics. The probability of a fluctuation leading to a signal with 3.9σ significance or more in the mass range 1500–1560 MeV and with a Gaussian width in the range 1.5–12 MeV, was found to be 6×10^{-5}. The same exercise was carried out using the background plus the 1465 MeV Gaussian as the starting distribution, and the probability was found to be about a factor of ten lower.

Table 1
Fit results for $Q^2 > 20$ GeV^2

Fit		Gaussian + Bkg.	2 Gaussians + Bkg.
χ^2/ndf	$M \leqslant 1700$ MeV	51/47	35/44
Peak 1	mass (MeV)	–	1465.1 ± 2.9
	width (MeV)	–	15.5 ± 3.4
	events	–	368 ± 121
Peak 2	mass (MeV)	1522.2 ± 1.5	1521.5 ± 1.5
	width (MeV)	4.9 ± 1.3	6.1 ± 1.6
	events	155 ± 40	221 ± 48

The Gaussian function was replaced by a Breit–Wigner function convoluted with a Gaussian to describe the peak near 1522 MeV. The width of the Gaussian distribution was fixed to the experimental resolution to obtain an estimate of the intrinsic width of the signal. The extracted width was $\Gamma = 8 \pm 4$(stat.) MeV.

The fit was repeated for different values of the minimum Q^2 cut. Above $Q^2 \approx 10$ GeV^2 both the signal and background are consistent with having a $1/Q^4$ dependence, similar to the inclusive cross section. A MC study in which Σ^+ particles were modified to have a mass of 1530 MeV and artificially forced to decay to $K^0_S p(\bar{p})$ indicated that, at low Q^2, the impact of detector acceptance on the visible cross section is important; for $Q^2 < 10$ GeV^2 the number of selected candidates rises more slowly than $1/Q^4$, as well as more slowly than the background. Such acceptance effects may be the reason for the absence of a clear signal at low Q^2 and high W. However, this suppression of the signal may also be related to the unknown production mechanism of the signal.

The invariant-mass spectrum was investigated for the $K^0_S p$ and $K^0_S \bar{p}$ samples separately. The result is

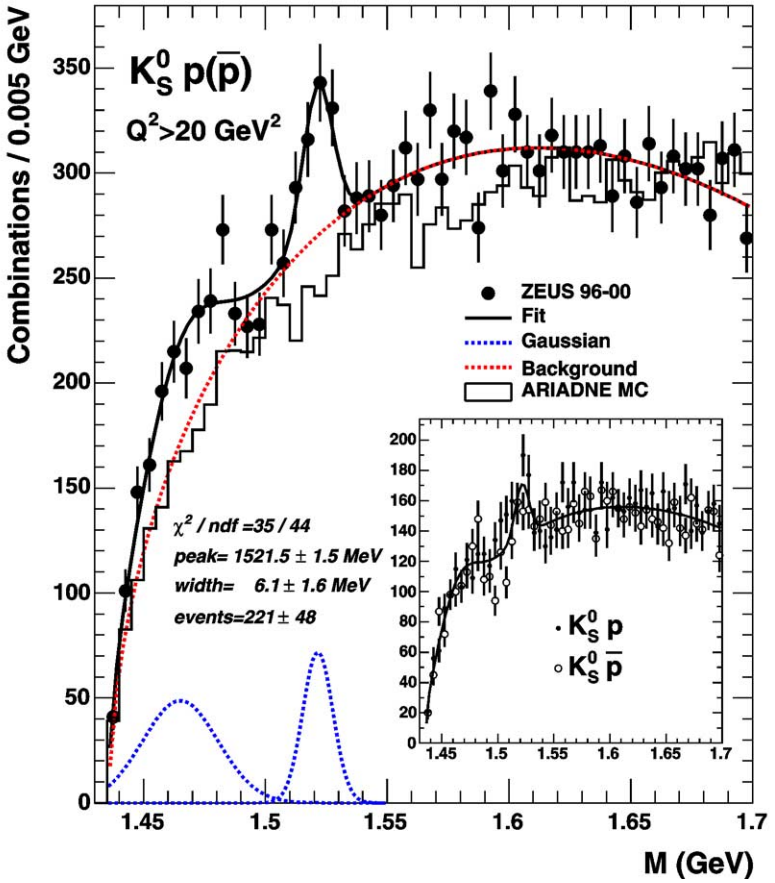

Fig. 4. Invariant-mass spectrum for the $K^0_S p(\bar{p})$ channel for $Q^2 > 20$ GeV^2, with other cuts as in Fig. 3. The solid line is the result of a fit to the data using a three-parameter background function plus two Gaussians (see text). The dashed lines show the Gaussian components and the dotted line the background according to this fit. The histogram shows the prediction of the ARIADNE MC simulation normalised to the data in the mass region above 1650 MeV. The inset shows the $K^0_S\bar{p}$ (open circles) and the $K^0_S p$ (black dots) candidates separately, compared to the result of the fit to the combined sample scaled by a factor of 0.5.

shown as an inset in Fig. 4 for $Q^2 > 20$ GeV^2, compared to the fit to the combined sample scaled by a factor of 0.5. The results for two decay channels are compatible, though the number of $K^0_S\bar{p}$ candidates is systematically lower. The mass distributions were fitted using the same function as the combined sample and gave statistically consistent results for the peak position and width (not shown). The number of events in the $K^0_S\bar{p}$ channel is 96 ± 34. If the signal corresponds to the Θ^+, this provides the first evidence for its antiparticle.

If an isotensor state is responsible for the signal, a Θ^{++} signal might be expected in the K^+p spectrum [22]. The $K^\pm p(K^\pm\bar{p})$ invariant mass spectra were investigated for a wide range of minimum Q^2 values, identifying proton and charged kaon candidates using dE/dx in a kinematic region similar to that used in the $K^0_S p(\bar{p})$ analysis. No peak was observed in the K^+p spectrum, while a clean 10σ signal[46] was observed in the K^-p spectrum at 1518.5 ± 0.6(stat.) MeV, corresponding to the $\Lambda(1520)D_{03}$. Performing a fit using a Gaussian fixed to the detector resolution convoluted with a Breit–Wigner gives

[46] The signal for $\bar{\Lambda}(1520)$ in the $K^+\bar{p}$ spectrum has the same number of events and significance as the $\Lambda(1520)$ signal in the K^-p spectrum.

an intrinsic width of 13.7 ± 2.1(stat.) MeV, consistent with the PDG value of 15.6 ± 1.0 MeV [6].

8.1. Systematic checks

A number of checks have been carried out to study possible reflections from known states and to verify the robustness of the 1522 MeV peak.

Tracks from the proton band within twice the width of the K^* peak were removed. According to a MC calculation, this cut increased the purity of the proton sample by 15% and reduced the statistics by a factor of 2.5. The resulting peak position was unchanged.

The energy of the proton candidates was required to be higher than that of the K^0_S, to reduce the combinatorial background [23]. Using this cut and the K^*-rejection cut, a peak may be seen in the mass spectrum even in the $Q^2 > 1$ GeV^2 sample. However, this combination of cuts leads to a complicated background shape, making the significance and the mass of the signal difficult to evaluate.

The $K^0_S K^\pm$ invariant mass was reconstructed from the data using the $K^\pm$ mass hypothesis for proton candidates, to see whether D_S decays contribute to the signal. It was verified that heavy-flavour particles cannot contribute to this spectrum if $M(K^0_S p(\bar{p})) \leqslant 2000$ MeV.

The K^0_S candidates were combined with primary tracks in the region $dE/dx \leqslant 1.15$ mips and $p \leqslant 1.5$ GeV, where pions are expected to dominate over (anti)protons. The invariant mass was reconstructed using the same procedure as before, applying the proton-mass hypothesis for selected tracks. In addition, the mass distribution was calculated using the pion band of the dE/dx plot to select proton candidates, and by using proton and K^0_S candidates from different events. In none of these cases was any structure seen in the mass distribution.

The robustness of the peak was also checked by varying the event and track selections. The maximum momentum for the proton candidates was changed in a wide range from 1.2 GeV to 4.0 GeV. The dE/dx cut was varied in the range 1.1 to 1.3 mips. No change was seen in the peak position.

8.2. Systematic uncertainties

The systematic uncertainties on the peak position and the width, determined from the fit shown in Fig. 4, were evaluated by changing the selection cuts and the fitting procedure. The largest uncertainties on the peak position and the Gaussian width for each check are given in parentheses (in MeV). The following systematic studies have been evaluated:

- the DIS selection cuts were found to have a negligible effect on the peak position. The largest uncertainty was found by raising the Q^2 cut to 30 GeV^2 $(+0.8, +0.3)$;
- the 40-hit requirement for the proton candidates was not used $(+0.1, +1.5)$. The variations of the cuts on the tracks in the laboratory frame were found to have a negligible effect on the peak;
- the dE/dx cut was increased to 1.3 mips $(+0.6, -0.7)$. The maximum momentum of protons was varied within $1.3 - 4.0$ GeV $(^{-0.4}_{-0.5}, ^{+0.8}_{-0.3})$;
- the bin size was raised and lowered by 1 MeV $(^{-1.2}_{-0.4}, ^{+0.1}_{+0.6})$; the log-likelihood method was used for the fitting procedure instead of the χ^2 method (no change);
- the fit was made using only a single Gaussian $(+0.6, -1.2)$, or with three Gaussians $(-0.1, +0.7)$; the background function was changed to a third-order polynomial $(+0.6, 0.0)$;
- the CTD momentum calibration uncertainty on the peak position was calculated from the mass measurements of K^0_S, Λ and K^*, as well as the Λ_c reconstructed in the $K^0_S p(\bar{p})$ decay channel $(^{+2.4}_{-0.8})$.

The overall systematic uncertainties of $^{+2.8}_{-1.7}$ MeV and $^{+2.0}_{-1.4}$ MeV on the peak position and the width were determined by adding the above uncertainties in quadrature.

9. Summary and conclusions

The $K^0_S p(\bar{p})$ invariant mass spectrum has been studied in inclusive deep inelastic ep scattering for a large range in the photon virtuality. For $Q^2 \gtrsim 10$ GeV^2 a peak is seen around 1520 MeV.

The peak position, determined from a fit to the mass distribution in the kinematic region $Q^2 \geqslant 20$ GeV^2, is $1521.5 \pm 1.5(\text{stat.})^{+2.8}_{-1.7}(\text{syst.})$ MeV, and the measured Gaussian width of $\sigma = 6.1 \pm 1.6(\text{stat.})^{+2.0}_{-1.4}(\text{syst.})$ MeV is above, but consistent with, the experimental reso-

lution of 2.0 ± 0.5 MeV. The number of events ascribed to the signal by this fit is 221 ± 48. The statistical significance, estimated from the number of events assigned to the signal by the fit, varies between 3.9σ and 4.6σ depending upon the treatment of the background. The probability of a similar signal anywhere in the range 1500–1560 MeV arising from fluctuations of the background is below 6×10^{-5}.

The results provide further evidence for the existence of a narrow baryon resonance consistent with the predicted Θ^+ pentaquark state with a mass close to 1530 MeV and a width of less than 15 MeV. Evidence for such a state has been seen by other experiments, although the mass reported here lies somewhat below the average mass of these previous measurements. In the Θ^+ interpretation, the signal observed in the $K^0_S\bar{p}$ channel corresponds to first evidence for an antipentaquark with a quark content of $\bar{u}\bar{u}\bar{d}\bar{d}\bar{s}$. The results, obtained at high energies, constitute first evidence for the production of such a state in a kinematic region where hadron production is dominated by fragmentation.

Acknowledgements

We thank the DESY Directorate for their strong support and encouragement. The remarkable achievements of the HERA machine group were essential for the successful completion of this work and are greatly appreciated. We are grateful for the support of the DESY computing and network services. The design, construction and installation of the ZEUS detector have been made possible owing to the ingenuity and effort of many people from DESY and home institutes who are not listed as authors.

References

[1] LEPS Collaboration, T. Nakano, et al., Phys. Rev. Lett. 91 (2003) 012002;
SAPHIR Collaboration, J. Barth, et al., Phys. Lett. B 572 (2003) 127;
CLAS Collaboration, V. Kubarovsky, et al., Phys. Rev. Lett. 91 (2003) 252001;
CLAS Collaboration, V. Kubarovsky, et al., Phys. Rev. Lett. 92 (2004) 032001;
CLAS Collaboration, V. Kubarovsky, et al., Phys. Rev. Lett. 92 (2004) 049902, Erratum.
[2] D. Diakonov, V. Petrov, M.V. Polyakov, Z. Phys. A 359 (1997) 305.
[3] DIANA Collaboration, V.V. Barmin, et al., Phys. At. Nucl. 66 (2003) 1715;
A.E. Asratyan, A.G. Dolgolenko, M.A. Kubantsev, hep-ex/0309042;
SVD Collaboration, A. Aleev, et al., hep-ex/0401024;
HERMES Collaboration, A. Airapetian, et al., Phys. Lett. B 585 (2004) 213;
COSY-TOF Collaboration, M. Abdel-Bary, et al., hep-ex/0403011.
[4] NA49 Collaboration, C. Alt, et al., Phys. Rev. Lett. 92 (2004) 042003.
[5] H1 Collaboration, A. Aktas, et al., hep-ex/0403017.
[6] Particle Data Group, K. Hagiwara, et al., Phys. Rev. D 66 (2002) 010001.
[7] ZEUS Collaboration, U. Holm (Ed.), The ZEUS Detector, Status report (unpublished), DESY (1993), available on http://www-zeus.desy.de/bluebook/bluebook.html.
[8] N. Harnew, et al., Nucl. Instrum. Methods A 279 (1989) 290;
B. Foster, et al., Nucl. Phys. B (Proc. Suppl.) B 32 (1993) 181;
B. Foster, et al., Nucl. Instrum. Methods A 338 (1994) 254.
[9] ZEUS Collaboration, J. Breitweg, et al., Phys. Lett. B 481 (2000) 213;
ZEUS Collaboration, J. Breitweg, et al., Eur. Phys. J. C 18 (2001) 625.
[10] M. Derrick, et al., Nucl. Instrum. Methods A 309 (1991) 77;
A. Andresen, et al., Nucl. Instrum. Methods A 309 (1991) 101;
A. Caldwell, et al., Nucl. Instrum. Methods A 321 (1992) 356;
A. Bernstein, et al., Nucl. Instrum. Methods A 336 (1993) 23.
[11] A. Bamberger, et al., Nucl. Instrum. Methods A 382 (1996) 419;
S. Magill, S. Chekanov, in: B. Aubert, et al. (Eds.), Proceedings of the IX Int. Conference on Calorimetry, Annecy, 9–14 October, 2000, in: Frascati Physics Series, vol. 21, 2001, p. 625.
[12] A. Bamberger, et al., Nucl. Instrum. Methods A 401 (1997) 63.
[13] J. Andruszków, et al., Preprint DESY-92-066, DESY, 1992;
ZEUS Collaboration, M. Derrick, et al., Z. Phys. C 63 (1994) 391;
J. Andruszków, et al., Acta Phys. Pol. B 32 (2001) 2025.
[14] L. Lönnblad, Comput. Phys. Commun. 71 (1992) 15.
[15] A. Kwiatkowski, H. Spiesberger, H.-J. Möhring, Comput. Phys. Commun. 69 (1992) 155;
W. Buchmüller, G. Ingelman (Eds.), Proc. Workshop Physics at HERA, DESY, Hamburg, 1991.
[16] H. Spiesberger, HERACLES and DJANGOH: Event Generation for *ep* Interactions at HERA Including Radiative Processes, 1998, available on http://www.desy.de/~hspiesb/djangoh.html.
[17] B. Andersson, et al., Phys. Rep. 97 (1983) 31.
[18] T. Sjöstrand, Comput. Phys. Commun. 82 (1994) 74.

[19] R. Brun, et al., GEANT3, Technical Report CERN-DD/EE/84-1, CERN, 1987.
[20] F. Jacquet, A. Blondel, in: U. Amaldi (Ed.), Proceedings of the Study for an *ep* Facility for Europe, Hamburg, Germany, 1979, p. 391, also in preprint DESY 79/48.
[21] H. Abramowicz, A. Caldwell, R. Sinkus, Nucl. Instrum. Methods A 365 (1995) 508.
[22] S. Capstick, et al., Phys. Lett. B 570 (2003) 185.
[23] B. Levchenko, hep-ph/0401122.